

# keV RESONANCE NEUTRON CAPTURE IN IRON

By M. J. KENNY\*

[Manuscript received 3 August 1971]

## Abstract

Resonance behaviour has been observed at a number of neutron energies between 5 and 90 keV. Transition intensities show strong fluctuations with neutron energy. The presence of p- and/or d-wave capture is inferred from the occurrence of transitions to high spin states. A distribution of reduced widths for low spin states suggests some departure from statistical processes, particularly for the strongest transitions.

## I. INTRODUCTION

Extensive studies have been made of keV neutron capture in a sample of natural iron for the neutron energy range 5–100 keV. Previous measurements have been reported by Bird, Kenny, and Allen (1969) and Kenny, Bird, and Allen (1969) but this paper presents results obtained with improved experimental techniques and discusses all the available data. The experiment was one of a series for the mass region  $A = 40$ –70 undertaken in this laboratory to obtain increased understanding of the neutron capture process. Capture by iron isotopes is of interest because of the peaks in the s- and d-wave strength functions near mass 55. The thermal capture spectrum for iron is well known (Groshev *et al.* 1964; Bartholomew *et al.* 1967; Wasson *et al.* 1968), and Bird (1968) has obtained keV capture spectra using NaI detectors. The present experiment used both a high resolution Ge(Li) detector and a large NaI detector. Individual resonances or groups of resonances were resolved and their energies were found by observing the shift of the  $\gamma$ -ray energy above the value which might be expected in thermal capture and also by time of flight methods.

A resonance for capture by  $^{56}\text{Fe}$  exists at 1167 eV and has been studied extensively (Block 1964; Wasson *et al.* 1968; Asami, Moxon, and Stein 1969; Chrien, Bhat, and Wasson 1970). It has been designated as p-wave and has shown evidence of a major enhancement of electric quadrupole transitions.

## II. EXPERIMENTAL METHOD

Natural iron contains 91.66%  $^{56}\text{Fe}$  and 5.82%  $^{54}\text{Fe}$ . The thermal capture cross sections of both are about 2.7 barns, whilst the 30 keV averaged capture cross sections for  $^{56}\text{Fe}$  and  $^{54}\text{Fe}$  respectively are 13.5 and 34 mb. Following capture by  $^{54}\text{Fe}$ , the transition to the ground state of  $^{55}\text{Fe}$  has an energy of 9296 keV and in  $^{56}\text{Fe}$  capture, the  $^{57}\text{Fe}$  ground state  $\gamma$ -ray has an energy of 7643 keV. The data presented here were obtained from a number of different measurements:

- (1) a 10 cm<sup>3</sup> coaxial Ge(Li) detector, covering the energy range 6.1–9.4 MeV;
- (2) the same detector covering 4.5–7.8 MeV;

\* A.A.E.C. Research Establishment, Private Mail Bag, Sutherland, N.S.W. 2232.

- (3) the same detector covering 1.0–5.0 MeV; and
- (4) a 20 cm by 15 cm NaI crystal covering the restricted range 7.4–7.8 MeV, but with better timing resolution.

These measurements gave a significant improvement over previous measurements in both  $\gamma$ -ray and neutron energy resolution.

The A.A.E.C. 3 MeV pulsed Van de Graaff was used to irradiate a lithium target at a proton energy 17 keV above the neutron threshold. For the Ge(Li) measurements, run times of up to 80 hr were required with about  $8 \mu\text{A}$  of average beam current. For the NaI data, the beam was klystron bunched to a width of 1 ns and an average current of  $5 \mu\text{A}$  was used for 8 hr. Neutron time of flight and  $\gamma$ -ray spectra were simultaneously analysed using an 8K memory PDP-7 computer.

The apparatus layout for Ge(Li) measurements, referred to as "cone geometry", has been described previously (Allen, Kenny, and Sparks 1968; Allen, Bird, and Kenny 1969). The cone was made of  $\text{B}_4\text{C}$  in paraffin. An 8 cm lead plug was placed immediately forward of the detector which was surrounded by a 0.8 cm lead sleeve. The lead considerably reduced the 0.5 MeV  $\gamma$ -flux from (p,  $\gamma$ ) events in the lithium target and from decay of  ${}^7\text{Be}$  formed in the  ${}^7\text{Li}(\text{p}, \text{n}){}^7\text{Be}$  reaction and also the  $\gamma$ -flux from neutron capture in the boron. The floor was covered with 10 cm of borated paraffin to a radius of 3 m to reduce the effects of neutron scattering and capture by the reinforced concrete. These improvements halved the background rate of earlier cone geometry experiments. The NaI measurements were made with the target in the centre of the neutron flux and the detector at  $90^\circ$ . Electronics and data handling were essentially the same as for the Ge(Li) measurements.

The PDP-7 computer was programmed to permit the selection of variable width time windows and the accumulation of pulse height spectra for these ranges. By sacrificing one of the six 1024-channel windows, the time spectrum corresponding to the sum of all the pulse height windows could be accumulated simultaneously.

For the Ge(Li) measurements the sample consisted of 50 kg of mild steel in dished annular form, 50 cm diameter. This shape reduced variations in the 50 cm flight path to  $\pm 1.5$  cm, corresponding to the thickness of the dish. Impurities such as carbon made no observable contribution to the spectra. The effectiveness of the outer regions of the sample in contributing to the count rate is reduced by

- (1) lower neutron intensity at the high neutron emission angles,
- (2) increased distance between the capture target and the detector, and
- (3) absorption of  $\gamma$ -rays by the iron.

It has been shown (R. J. Sparks, personal communication) that this last absorption is relatively independent of  $\gamma$ -ray energy between 6 and 10 MeV, but increases by up to 30% at 2 MeV. Corrections for this effect were made by thermalizing the neutron beam and comparing the observed spectrum with the thermal data (Groshev *et al.* 1964), thereby obtaining an effective efficiency calibration for the cone geometry. The target size and beam current chosen provided several thousand counts in the strongest peaks and a few hundred in the weakest observable peaks.

The  ${}^7\text{Li}(\text{p}, \text{n}){}^7\text{Be}$  kinematics are such that neutrons between 5 and 90 keV reach the capture sample. The intensity versus energy distribution of the neutrons has

been calculated and shows that the maximum intensity occurs at about 46 keV and the energies at which the intensity falls to half this maximum are 12 and 76 keV. From 32 to 64 keV the relative intensity varies by less than 5%.

For the Ge(Li) measurements, the beam pulse width was about 15 ns and the time resolution of the Ge(Li) detector was  $\sim 20$  ns. Hence the overall time resolution was  $\sim 25$  ns. The time spectrum was used to route the pulse height spectra into one of six windows corresponding to the preselected neutron energy groups. The timing spread (equivalent to about half a window width) had the effect of smearing a peak into adjacent windows, making data interpretation more difficult.

The neutron resonance energy is generally deduced by observing the shift in  $\gamma$ -ray energy above the expected thermal capture value, but this becomes difficult when there are two  $\gamma$ -rays whose energy difference is close to the resolution limit and the resonance spacing is of the same order. For example, a 28 keV neutron captured by  $^{56}\text{Fe}$  gives a 7671 keV transition to the ground state while a 36 keV neutron gives a 7665 keV transition to the first excited state. In the present experimental arrangement these cannot be separated either by pulse height or time of flight.

A constant fraction timing discriminator was used with the 20 cm by 15 cm NaI detector and the proton beam was klystron bunched to 2 ns. Over a dynamic range of several MeV, the timing resolution of the system was 3.5 ns. Data were obtained with a target of 850 g of iron in sheet form. The  $\gamma$ -ray energy range was 7.4–7.8 MeV and the flight path was 50 cm. The behaviour of the ground and 14 keV state doublet in  $^{57}\text{Fe}$  was studied by combining the high resolution pulse height data from the Ge(Li) work with the high resolution neutron energy data from the NaI experiment.

The evaporated lithium target was pumped to a pressure of  $10^{-7}$  torr by a  $15 \text{ l s}^{-1}$  Vacion pump and was separated from the main beam line by a high pumping impedance. The neutron yield was continuously monitored by a long counter placed in the neutron cone several metres beyond the capture target.

Background counts have both time-dependent and time-independent components, so that the technique of using a time window away from the neutron flux to monitor the background is only partially correct. Tests with different thickness targets of carbon, cadmium, and aluminium have shown that the time-dependent background can be calculated with reasonable accuracy. The most satisfactory count to background ratio was obtained at a proton energy about 17 keV above the  $^7\text{Li}(p, n)$  threshold.

### III. EXPERIMENTAL RESULTS

#### (a) Capture by $^{54}\text{Fe}$

The low isotopic abundance of  $^{54}\text{Fe}$  restricts the information that can be derived for capture by this isotope when a natural sample is used. However, because of the higher binding energy, capture by  $^{54}\text{Fe}$  leading to the ground or any of the first four excited states of  $^{55}\text{Fe}$  results in higher energy  $\gamma$ -rays than can be obtained after capture by  $^{56}\text{Fe}$ , and hence these transitions may be seen in the pulse height spectrum. Only the first series of measurements covered this energy range and the summed keV capture spectrum is presented in Figure 1. The intensities are summarized in Table 1(a) for the neutron energy regions 20–40 and 40–75 keV.

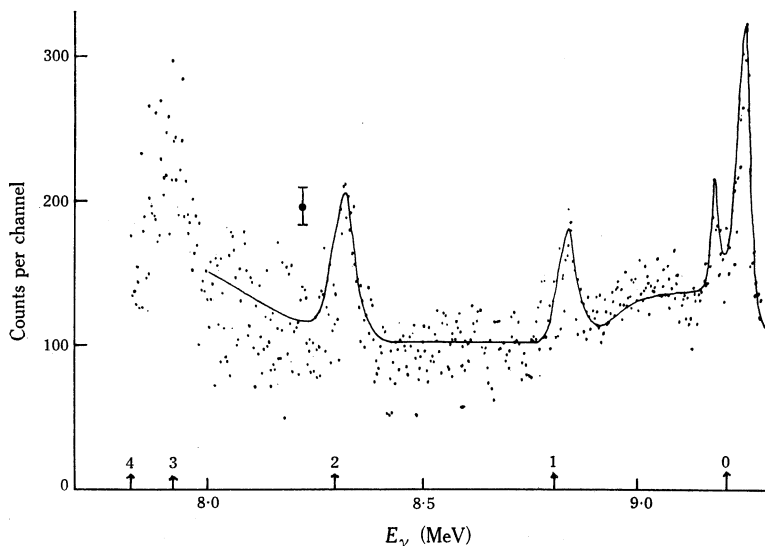


Fig. 1.—Summed  $\gamma$ -ray spectrum following keV neutron capture by  $^{54}\text{Fe}$ . The arrows indicate levels of  $^{55}\text{Fe}$  listed in Table 1(a). The lower section of the curve includes a full energy peak due to capture by  $^{56}\text{Fe}$ .

#### (b) Capture by $^{56}\text{Fe}$

Pulse height spectra were obtained for six time intervals. Five of these correspond to different neutron energy groups and the sixth covers a region beyond the expected flight times of the keV neutrons. A typical time of flight spectrum obtained with the Ge(Li) detector is shown in Figure 2(a) with the digital window (DW) positions indicated. Mean neutron energies for the windows DW5–1 are 15, 22, 35, 52, and 72 keV respectively. The region between DW5 and DW6 is largely due to scattered background. The time resolution is  $\sim 25$  ns as seen by the width of the  $(p, \gamma)$  peak. Additional neutron time spread occurs due to the 3 cm sample thickness. The time of flight spectrum, using the NaI detector, a thin sample, and 4 ns timing resolution, is shown in Figure 2(b). The improved timing resolution shows all the known resonances in this region (Hockenbury *et al.* 1969). The proton energy above threshold and the experimental geometry are such that the neutron energy range in Figure 2(a) extends to 90 keV, while that in Figure 2(b) cuts off at 60 keV.

The keV capture spectra for four neutron energy groups above 20 keV are shown in Figure 3. The spectrum obtained by summing the digital windows over neutron energy is shown in Figure 4 together with a thermal comparison spectrum obtained by paraffin moderation of the neutron flux. Very little resonance capture is seen at neutron energies below  $\sim 20$  keV. The relative transition intensities for the various digital windows together with the thermal intensities (Groshev *et al.* 1964) and the 1167 eV intensities (Wasson *et al.* 1968) are presented in Table 1(b). For the ground and 14 keV states, the 4 ns resolution timing data (NaI) and the high resolution pulse height data (Ge(Li)) have been combined to derive the data for the individual resonances given in Table 2. For the other states data are presented in Table 1(b) for four neutron energy groups.

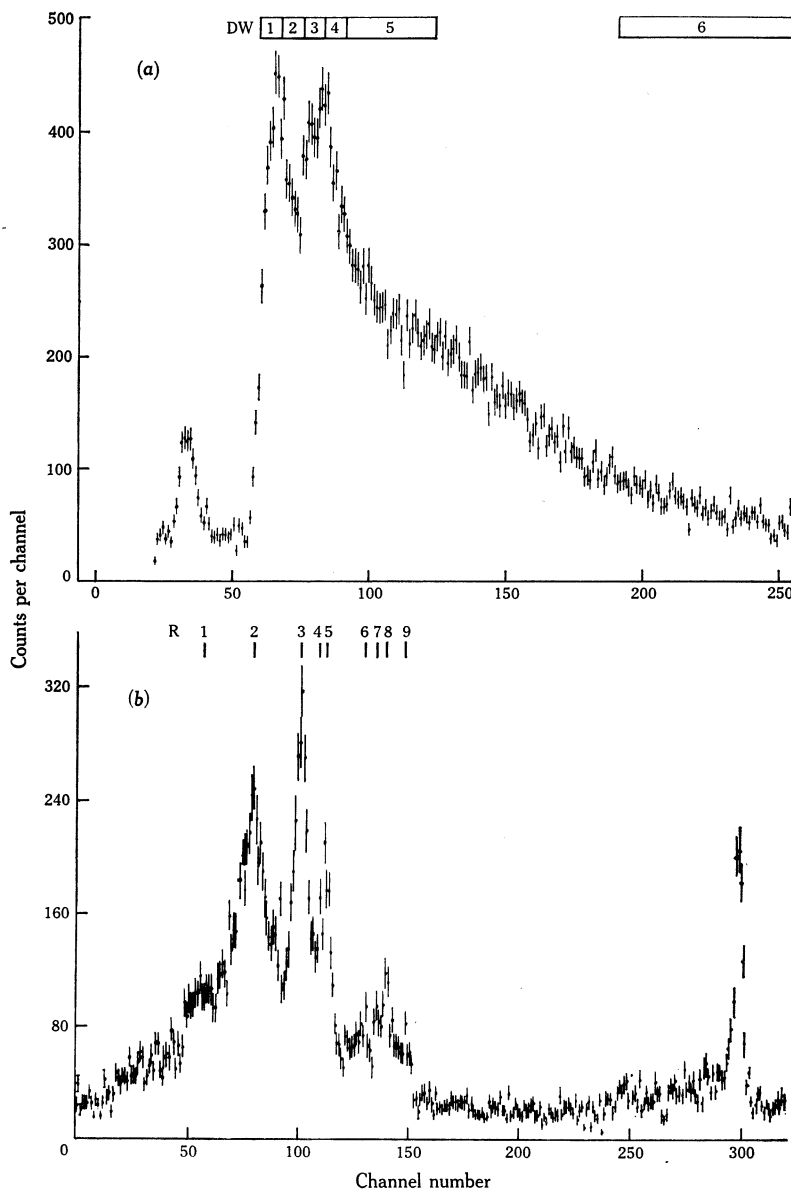


Fig. 2.—Time of flight spectra for neutron capture by natural iron obtained with (a) a Ge(Li) detector and a 50 kg sample and (b) an NaI detector and an 850 g sample. The improved timing resolution in (b) shows all the known resonances in this region: R1, 22.7; R2, 27.7; R3, 34.1; R4, 36.6; R5, 38.3; R6, 45.8; R7, 51.9; R8, 53.3; R9, 59.0 keV.

Normalization for both thermal and keV capture is on the assumption that transitions to states below 3500 keV account for  $(85 \pm 15)\%$  of all transitions. This is similar to the normalization used by Bartholomew *et al.* (1967). The level scheme of  $^{57}\text{Fe}$  is not clearly defined above 2500 keV excitation; there are numerous closely spaced levels which are partly confused by minor variations in (d, p) data. The levels

TABLE 1  
RELATIVE INTENSITIES FOR keV CAPTURE IN IRON

Normalization  $\Sigma I_i(\text{keV}) = \Sigma I_i(\text{thermal}) = 85 \pm 15$  photons per 100 captures in isotope

$E_f$ (d, p)* (keV)	$l_n$	$J_i^\pi$	$E_\gamma$ Thermal† (keV)	Intensity per 100 Captures for Different Neutron Energy Groups (keV)				Sum (20-75)			
				Thermal	20-40	40-75					
(a) Capture in $^{54}\text{Fe}$											
$^{54}\text{Fe}$	0	1	3/2 <sup>-</sup>	9296	58	37	43	40			
	1	1	1/2 <sup>-</sup>	8886	11	9	25	23			
	2	3	5/2 <sup>-</sup>	8273‡		36	10	17			
	3	3	5/2 <sup>-</sup> 7/2 <sup>-</sup>	7884‡		3	7	5			
	4		7/2 <sup>-</sup>	7723	0.1	0	0	0			
	1925	1		7377							
	2058	1	3/2 <sup>-</sup>	7248	1.6						
	2151	3									
	2478	1			1.9						
	2546				0.6						
	2585	4									
	3035		3/2 <sup>-</sup>	6266	2.9						
	Others				8.8						
(b) Capture in $^{56}\text{Fe}$											
					Thermal	1.17	26	36	52	72	Sum (20-75)
$^{56}\text{Fe}$	0	1	1/2 <sup>-</sup>	7643	21.5	18.3	32.1	19.8	8.4	18.9	20.6
	1	1	3/2 <sup>-</sup>	7629	21.5	35.8	21.0	33.2	10.9	24.7	23.2
	2	3	5/2 <sup>-</sup>	7507‡		2.5	0.9	1.0	6.8	13.4	5.0
	3	1	3/2 <sup>-</sup>	7277	5.3	0.8		3.7	16.7	11.0	6.6
	4		5/2 <sup>-</sup>	6937‡			2.3	8.2	5.5	2.9	3.4
	5			6635‡						1.0	0.3
	6			6445‡		0.9					
	7	1	3/2 <sup>-</sup>	6379	0.6	13.1	7.1	10.2	5.9		5.3
	8	(1)		6285‡						3.2	1.0
	9	1	3/2 <sup>-</sup>	6018	8.5	1.3	5.0	6.8	15.2	4.5	6.4
	10	1	3/2 <sup>-</sup>	5920	8.3	2.9			3.6	4.2	1.8
	11	(2)		5649‡							
	12	(3)		5521‡							
	13			5433‡							
	14	1		5418‡							
	15			5183‡							
	16	4		5134‡							
	17	2		5087‡							
	18	4		5067‡							
	19	1		5043‡							
	20	} 1	(3/2 <sup>-</sup> )	4950	0.8	2.1	9.4				3.9
	2700 (group)										
	21		3/2 <sup>-</sup>	4810	1.9	0.2		3.0	11.2	1.5	3.5
	22			4723‡			7.7				4.2
	23			4680	0.4						
	24	1		4462	0.5	2.1					
	25	(1)		4405	1.4	0.7					
	26	1		4274	0.4						
	27	1	3/2 <sup>-</sup>	4217	3.3	0.2					
	28			4014	0.4						
	29		1/2 <sup>-</sup>	3855	1.2	0.6					
	30			3792	0.3						

TABLE 1(b) (Continued)

$E_f$ (d, p)* (keV)	$l_n$	$J_f^\pi$	$E_\gamma$ Thermal† (keV)	Intensity per 100 Captures for Different Neutron Energy Groups (keV)								
				Thermal	1-17	26	36	52	72	Sum (20-75)		
31			3778									
32			3665									
33	1		3504									
34	2		3489									
35			3440									
36			3416									

Capturing state:

1/2<sup>+</sup>; 1/2<sup>-</sup>, 3/2<sup>-</sup>; 1/2<sup>+</sup> s or 1/2<sup>-</sup>, 3/2<sup>-</sup> p or 3/2<sup>+</sup>, 5/2<sup>+</sup> d\* Bartholomew *et al.* (1967).† Groshev *et al.* (1964).‡ Expected  $\gamma$ -ray energy in thermal capture deduced from (d, p) data.

TABLE 2

GROUND AND FIRST EXCITED STATE DATA FROM TABLE 1(b) WITH RESONANCES RESOLVED

$E_f$ (d, p) (keV)	$l_n$	$J_f^\pi$	$E_\gamma$ Thermal (keV)	Relative Intensity for Different Neutron Resonances (keV)								
				22.7	27.7	34.1	36.6 to 38.3	45.8 to 53.3	51.9 to 59	72	Sum (20-75)	
0	1	1/2 <sup>-</sup>	7643	4.8	27.2	9.9	7.5	2.5	6.0	2.4	18.9	20.6
14	1	3/2 <sup>-</sup>	7629	4.8	16.2	19.7	11.0	2.5	8.5	2.4	24.8	23.2

used were those indicated in the thermal capture survey (Bartholomew *et al.* 1967) and in the thermal results (Groshev *et al.* 1964).

The intensities summed over neutron energy obtained in the present experiment may be compared with those obtained at Oak Ridge (Bird 1968) using NaI detectors. Table 3 shows this comparison for <sup>56</sup>Fe capture. Minor discrepancies exist, but these are almost certainly due to the improved resolution of the Ge(Li) detector and uncertainties in efficiency corrections.

Peak areas were derived by the fitting of Gaussian shapes to the experimental points using the PDP-7 computer, allowance being made for skew on the leading edge of the peaks. The doublet was analysed by fitting Gaussians to the background spectrum and then using the same widths and shapes to fit the minimum number of Gaussians to the complex peaks observed in the keV spectra. The NaI resonance data were also taken into account. Individual relative intensities derived in the doublet may have errors of up to 20% when this technique is used. Statistical errors on peak areas vary between 3 and 10%.

It is seen from Figure 4 that the thermal spectrum shows  $\gamma$ -rays for excitations up to at least 3.5 MeV, whereas the keV spectrum shows no primary  $\gamma$ -rays to states above 3 MeV excitation. Since both spectra were obtained in the same geometry, it must be presumed that transitions to higher excitations play only a small role in keV capture. Since 70% of all transitions observed are to states below 1 MeV excitation, very few secondary  $\gamma$ -rays would be expected; these  $\gamma$ -rays are distinguished by their insensitivity to neutron energy. The peaks at 2686 and 2700 keV in Figure 4 are full energy peaks produced by decay through the 2700 keV state to the 14 keV and ground states.

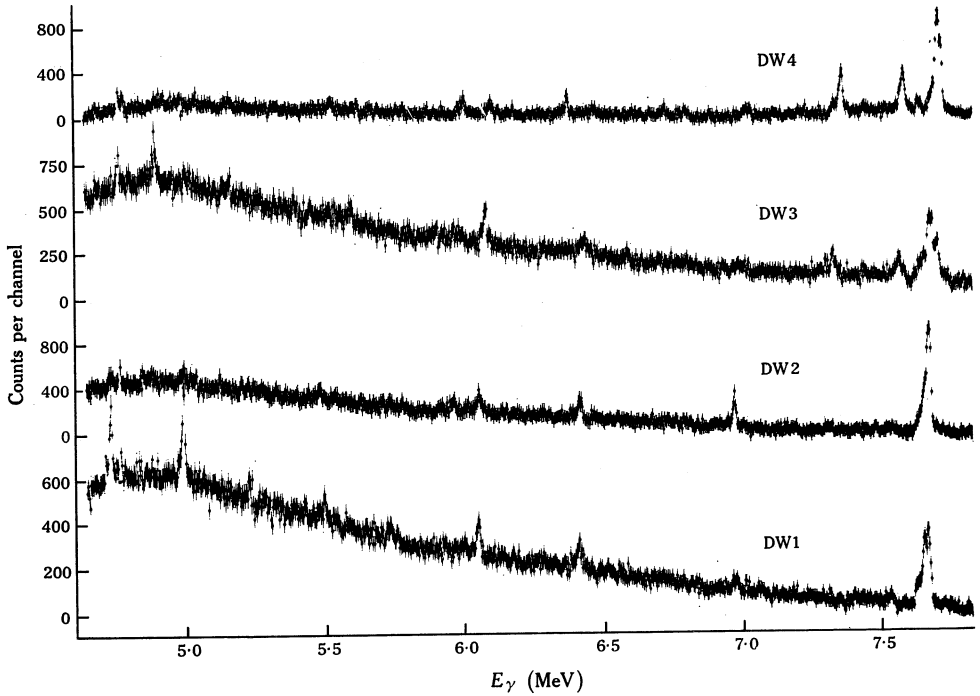


Fig. 3.—Gamma ray spectra from  $^{57}\text{Fe}$  following keV neutron capture for four neutron energy groups: DW1, 22; DW2, 35; DW3, 52; DW4, 72 keV.

TABLE 3  
COMPARISON OF DATA FROM Ge(Li) AND NaI DETECTORS FOR INTENSITIES OF TRANSITIONS IN  $^{57}\text{Fe}$   
Values normalized to 100%

$E_{\gamma}$ (keV)	Intensity of Transition (%)	
	Ge(Li) Detector	NaI Detector
0	24.3	39
14	27.2	
	} 51.5	
135	6	12
365	8	3
706	4	6
1260	6	7
1360	1.2	
	} 7.2	
1630	7.5	7.5
1730	2.1	
	} 9.6	
2680	4.6	12
2840	4.1	9.5
2920	5.0	
	} 9.1	

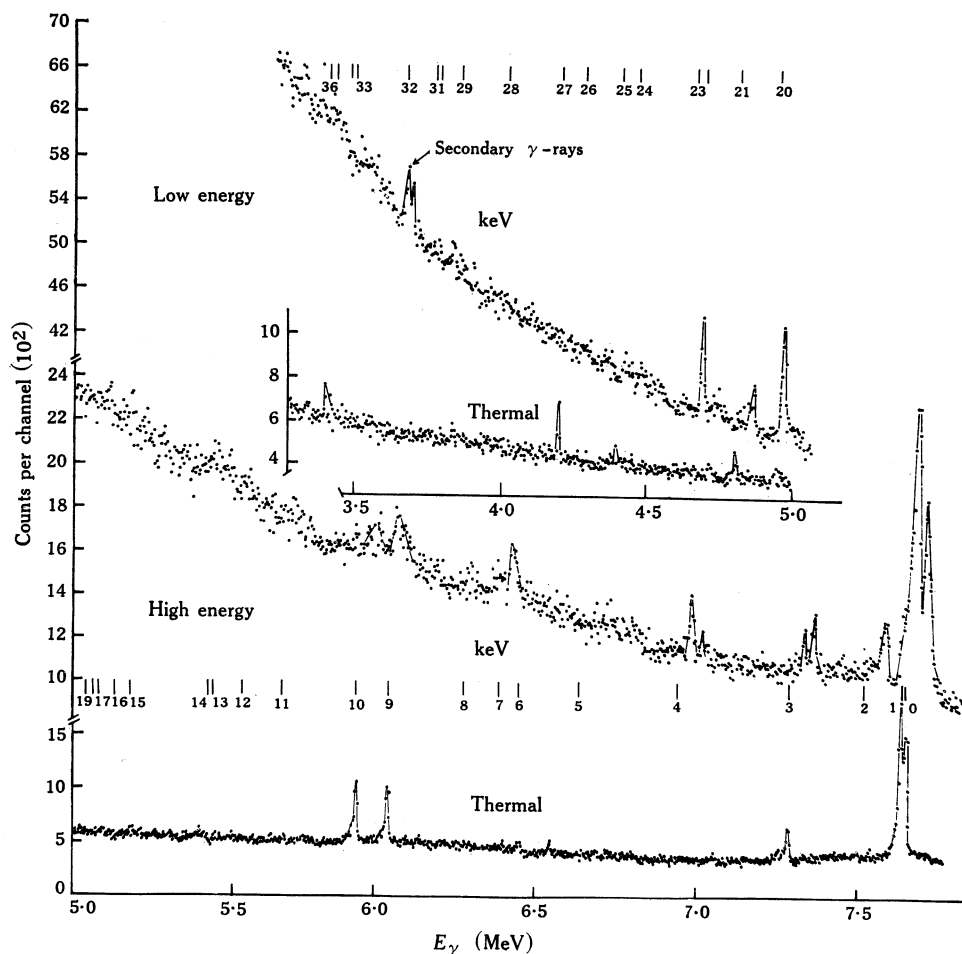


Fig. 4.—Gamma ray spectrum summed over neutron energy for keV capture by  $^{56}\text{Fe}$  together with a thermal comparison spectrum. The indicated levels in  $^{57}\text{Fe}$  are listed in Table 1(b).

#### IV. NEUTRON RESONANCES

##### (a) Resonance Locations

Neutron radiative capture in iron has been reported by Hockenbury *et al.* (1969) for the neutron energy range from 0.1 to 200 keV. Several previously unknown resonances were found and most were assigned as p-wave on strength function estimates. The reported resonances were:

$$^{54}\text{Fe} \text{ 7.82, 9.48, 14.4, 52 keV}$$

$$^{56}\text{Fe} \text{ 11.2, 22.7, 27.7, 34.1, 36.6, 38.3, 45.8, 51.9, 53.3, 59.0, 63.1, 72.6 keV}$$

The present Ge(Li) spectra show groups of resonances rather than individual ones, the energies at which intensities are strongest being close to the strongest resonances of Hockenbury *et al.*, namely, 15 and 50 keV for  $^{54}\text{Fe}$  and 27, 38, 52, and

72 keV for  $^{56}\text{Fe}$ . The  $^{56}\text{Fe}$  data, from the NaI improved timing experiment (Fig. 2(b)), are in excellent agreement with the results of Hockenbury *et al.*

Different  $l$ -wave resonances may exist close to one another in energy. These may not be resolvable by existing neutron or  $\gamma$ -ray techniques but may be distinguishable by the multipolarity of  $\gamma$ -ray transitions following the resonance capture. The strong resonance at 27.7 keV has been assigned as s-wave (Goldberg *et al.* 1966).

### (b) High Spin States

Both  $^{54}\text{Fe}$  and  $^{56}\text{Fe}$  target nuclei have spin and parity  $0^+$ , so that the possible  $J^\pi$  values of capture states for s-, p-, and d-wave neutrons are respectively  $1/2^+$ ,  $1/2^-$  or  $3/2^-$ , and  $3/2^+$  or  $5/2^+$ . Table 1 lists transitions to several states which are not seen in thermal capture. For  $^{54}\text{Fe}$  capture these states are at 933 keV ( $5/2^-$ ) and 1322 keV ( $5/2^-$ ,  $7/2^-$ ) and for  $^{56}\text{Fe}$  capture they are at 135 keV ( $5/2^-$ ), 706 keV ( $5/2^-$ ), and 1358 and 2920 keV (unassigned). Transitions to these states are not expected from thermal (s-wave) capture, since  $5/2^-$  requires M2 (or E3) and  $7/2^-$  requires E3 (or M4) transitions. At keV energies, the probability of p- and d-wave capture increases and  $5/2^-$  states can be reached by E2 or M1 transitions from p-wave, or E1 from d-wave capture. To reach  $7/2^-$  states requires E1 (or M2) transitions from d-wave capture or E2 (or M3) transitions from p-wave capture.

From their studies of the 1167 eV p-wave resonance for  $^{56}\text{Fe}$ , the symmetric nature of the results for spectra at  $90^\circ$  and  $135^\circ$  has led Wasson *et al.* (1968) and Chrien, Bhat, and Wasson (1970) to deduce a  $1/2^-$  capturing state. The strong transitions to the ground ( $1/2^-$ ) and first excited ( $3/2^-$ ) states seen in this resonance are thus M1 with reduced widths of the order of 20 Weisskopf units while the transition to the 135 keV  $5/2^-$  state is E2 with a strength of about 200 W.u.

The significance of high spin transitions following keV neutron capture in 11 even- $Z$  nuclei in the mass region  $A = 40-70$  has been discussed by Bird, Kenny, and Allen (1969). The simplest interpretation, based on expected reduced width values, assigns these to d-wave capture followed by E1 transitions; p-wave capture would involve reduced widths of many Weisskopf units and a major enhancement of M1 and E2 transitions. On the basis of the results of Wasson *et al.* (1968) and Chrien, Bhat, and Wasson (1970), however, the latter possibility cannot be neglected and whether the capture is p- or d-wave remains to be established.

In keV but not thermal capture by  $^{56}\text{Fe}$ , transitions are seen to the unassigned states at 1358 and 2920 keV and this implies that these are high spin states, the likely assignment being  $5/2^-$  or  $7/2^-$ . Alternatively, they may be positive parity states reached by electric dipole transitions from p-wave capture.

Since the 27.7 keV resonance is assigned as s-wave (Goldberg *et al.* 1966), high spin transitions would not be expected from this resonance. A weak transition is seen to the 135 keV state and a strong transition to the 2920 keV state at about this energy, implying either M2 transitions or a neighbouring higher  $l$ -wave resonance, the latter being more likely. The high spin transitions are stronger at 52 and 72 keV than at lower neutron energies and this suggests that these resonances are higher  $l$ -wave or that there are s-, p-, or d-wave resonances close to one another.

Hockenbury *et al.* (1969) argue that d-wave resonances are not significant since computation of the d-wave strength function for these yields a value that is an order

of magnitude larger than that expected from theory and the strength of the smallest observed resonance is adequate to account for the entire calculated d-wave strength function. If this interpretation is correct and the high spin transitions follow p-wave capture, then the present data show a major M1 enhancement.

(c) *Low Spin States*

Thermal capture by  $^{54}\text{Fe}$  is followed by transitions to the  $^{55}\text{Fe}$  ground state ( $3/2^-$ ) in 63% of all captures and for  $^{56}\text{Fe}$ , nearly 50% of all thermal captures lead to transitions to the ground ( $1/2^-$ ) or 14 keV ( $3/2^-$ ) states of  $^{57}\text{Fe}$ . While it is expected that  $l = 0$  capture would favour low spin transitions, these high energy transitions are amongst the strongest observed anywhere in the mass region 40–70. The other low spin states of  $^{55}\text{Fe}$  and  $^{57}\text{Fe}$  are populated to a much lesser extent. Strong primary transitions may be explained in terms of simple shell model configurations which favour E1 transitions. The strength of the same transitions for the 1167 eV resonance in  $^{56}\text{Fe}$  is more difficult to explain if it is p-wave capture, since M1 or E2 transitions are involved.

For both isotopes, the keV spectra also show strong transitions to low spin states, the average intensities over the neutron range being similar to those in thermal capture. Individual intensities fluctuate strongly as may be seen from Table 1. Generally, transitions to all low spin states are stronger than those to the high spin states discussed in the previous subsection. This implies that s-wave capture is still the strongest process in this mass region. Some of the low spin strength may be due to electric dipole transitions from d-wave capture. Since the s- and d-wave strength functions both have peaks near mass 60, strong contributions might be expected from them, whereas p-wave is less likely, its peaks being near mass 30 and 100. This situation can best be clarified by angular distribution studies which yield the spin value of the resonance.

## V. TRANSITION RATES AND REDUCED WIDTHS

Reduced widths for E1 and M1 transitions may be defined by the following formulae (Bartholomew 1961)

$$k(\text{E1}) = \Gamma'_\gamma(\text{E1})_{\text{obs}}/E^3 A^{\frac{3}{2}} D, \quad k(\text{M1}) = \Gamma'_\gamma(\text{M1})_{\text{obs}}/E^3 D,$$

where  $D$  is the average spacing of levels with the same spin and parity as the capturing state,  $E$  is the  $\gamma$ -ray energy in MeV, and  $\Gamma_\gamma$  is the level width in eV. Reduced widths may be calculated for all observed transitions, but are complicated by the possible occurrence of additional resonances with  $l$  values of 0, 1, or 2 at similar energies ( $\Delta E \lesssim 5$  keV). This has the effect of giving too low a value for a reduced width and is most likely to occur when the high spin transitions are involved. Assuming that low spin transitions are largely due to s-wave capture leading to E1 radiation, reduced widths were calculated for neutron energies where resonance behaviour was observed and also for the summed keV results for both isotopes. The values fluctuated strongly, but the average for  $k(\text{E1})$  was  $1.0 \times 10^{-3}$  W.u., which is close to the average of  $3 \times 10^{-3}$  W.u. (Bartholomew 1961) for all thermal transitions. The reduced widths are listed in Table 4.

For heavy nuclei, the distribution of the reduced neutron widths of a resonance, i.e. the widths associated with the probability of scattering, can be described by a  $\chi^2$  distribution with one degree of freedom ( $\nu = 1$ ). In the eV region of resonance capture  $\gamma$ -ray experiments, it has been shown that the partial radiative widths obey a similar distribution with  $1 \leq \nu \leq 2$ . This suggests that both decay modes are one-channel processes. A number of simplifying assumptions must be made to obtain a distribution from the present data.

TABLE 4

REDUCED WIDTHS OF OBSERVED TRANSITIONS FOLLOWING keV NEUTRON CAPTURE IN IRON

$E_t$ (keV)	$E_\gamma$ Thermal (keV)	Reduced Widths ( $10^{-3}$ W.u.) for Different Neutron Energy Groups (keV)				Sum (20-75)
		20-40	40-75			
(a) Capture in $^{54}\text{Fe}$						
0	9296	0.47	0.61			0.55
413	8886	0.13	0.38			0.34
933	8273	0.62	0.20			0.33
1322	7844	0.06	0.16			0.16
(b) Capture in $^{56}\text{Fe}$						
		26	39	52	72	Sum (20-75)
0	7643	2.8	1.7	0.8	1.6	1.8
14	7629	1.9	3.0	0.9	2.2	2.0
135	7507	0.1	0.1	0.6	1.3	0.5
365	7277	0.0	0.4	1.7	1.1	0.7
706	6937	0.2	0.9	0.7	0.3	0.4
1008	6635	0.0	0.0	0.0	0.2	0.0
1264	6379	1.1	3.8	0.9	0.0	0.8
1358	6285	0.8	0.0	0.0	0.5	0.2
1629	6018	0.0	3.1	2.7	0.8	1.1
1727	5920	0.0	0.0	0.7	0.8	0.3
2700 (group) }	4950	3.1	0.0	0.0	0.0	1.3
2840	4810	0.0	1.0	4.1	0.5	1.2
2920	4723	2.9	0.0	0.0	0.0	1.5

For  $^{54}\text{Fe}$  capture, insufficient data are available. For  $^{56}\text{Fe}$  capture, resonance behaviour was observed in the four energy regions 26, 39, 52, and 72 keV, while the doublet behaviour was studied in considerable detail. Although data are available for the 1167 eV resonance (Wasson *et al.* 1968), they are omitted because of their p-wave nature. Of the 12 final states observed, only 8 are known to be low spin and so a population of 32 transitions is available. Figure 5(a) shows a distribution of the reduced widths calculated for these transitions together with fits for  $\nu = 1, 2, 4,$  and 16.

In plotting a distribution of reduced widths the method of normalization is of importance. In the above distribution, for a given neutron energy region, the sum of all low spin transitions has been normalized to 85. This makes no allowance for fluctuations in  $\Gamma_\gamma$  or for different intensities in the neutron groups. The normalization number of 85 is that used in Table 1(b), being the number of observed primary photons per 100 captures in the isotope. It is also assumed that all low spin transitions are due entirely to s-wave capture. Then, for a particular final state, the averaged normalized intensity over the neutron energy range is calculated and the ratios of each intensity to this mean are used to obtain the distribution.

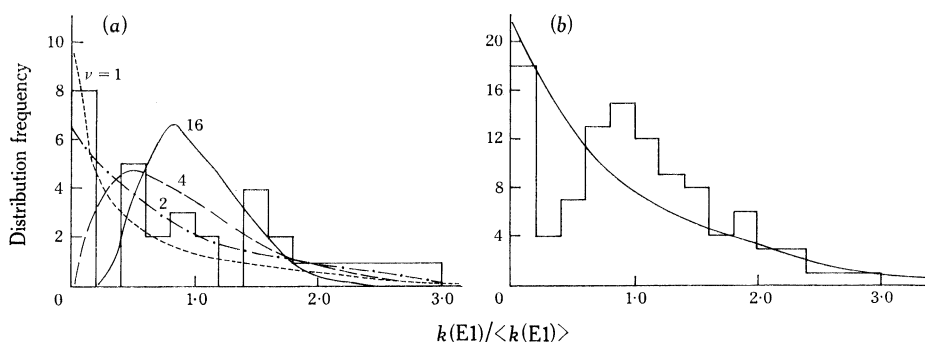


Fig. 5.—Distributions of reduced widths for transitions in (a)  $^{57}\text{Fe}$  and (b) even- $Z$  nuclei,  $A = 40$ – $70$ . Fits to the distribution are also shown in (a) for degrees of freedom  $\nu = 1, 2, 4$ , and  $16$ .

Alternative normalization methods were used. These involved normalization only on the two strongest transitions, use of the actual numbers of capture events seen in a particular resonance, or correction of these numbers for neutron intensity and energy distribution. No significant changes were made to the distribution by these normalizations. The main features of a high zero component, a bump in the region of  $k(E1)/\langle k(E1) \rangle \approx 1$ , and a scatter of high points were always retained.

The results of Hoekenbury *et al.* (1969) (Section IV(a)) show that there are at least 10 resonances in the neutron energy range covered and, since the data have been analysed for four neutron energy groups, a distribution similar to  $\nu = 2$  or  $3$  might be expected. With the limited data available, statistical variations of 50% or more might be expected in the distribution. The distribution of Figure 5(a) is similar to that for a low  $\nu$  ( $1 \leq \nu \leq 4$ ) but deviates near  $k(E1)/\langle k(E1) \rangle \approx 1$ . If the reduced widths to the two strongest states, i.e. the 2p states, are plotted separately then within the limits of available data the distribution resembles that for a higher value of  $\nu$  ( $\geq 4$ ) and the distribution for the remainder resembles  $\nu = 2$ . A similar conclusion was drawn by Allen (1970) using these data and also the 1167 eV resonance and lower energy data of Wasson *et al.* (1968). It appears that the behaviour for the weaker transitions is statistical while for the strong states there may be departure from statistical behaviour. Single-particle and direct capture effects could be presumed to affect these transitions.

Data are available (Allen, Bird, and Kenny 1969) for keV capture in other even- $Z$  nuclei in this mass region, namely  $^{41}\text{Ca}$ ,  $^{49}\text{Ti}$ ,  $^{53}\text{Cr}$ ,  $^{59}\text{Ni}$ , and  $^{61}\text{Ni}$ . Reduced

widths were calculated for all observed low spin transitions using the same assumptions as for the iron data. Since resonance spacings and experimental neutron energy ranges are similar for all nuclei, it is not unreasonable to combine the data in search of a trend. A population of over 100 reduced widths, comprising 40 from  $^{41}\text{Ca}$ , 32 from  $^{57}\text{Fe}$ , and the remainder approximately equally from the other four nuclei is obtained. Additional uncertainties arise because of the need for choosing partial radiation widths and level densities for each nucleus. This distribution is shown in Figure 5(b) and is similar to that for iron. The departure from a low  $\nu$  fit in the region  $k(E1)/\langle k(E1) \rangle \approx 1$  is more obvious. Separating the strong and weaker states gives a fit to high  $\nu$  values ( $4 \leq \nu \leq 16$ ) for the former and  $\nu = 2$  for the latter. The previous conclusions for iron are thus reinforced by the larger distribution.

In the case of titanium (Broomhall 1972), the only observed low spin transitions are those to the 2p states. An analysis of the distribution of reduced widths for resonances, allowing for variation in  $\Gamma_\gamma$ , shows a low  $\nu$  distribution. In this sense titanium behaves differently from iron and probably from other nuclei in this mass region.

## VI. CONCLUSIONS

The transitions to the 2p ground and first excited states which dominate thermal capture by  $^{56}\text{Fe}$  dominate averaged keV capture to a similar extent. Transitions to individual low spin states fluctuate strongly with neutron energy and are not distinguishable at an excitation of about 3 MeV.

For both  $^{54}\text{Fe}$  and  $^{56}\text{Fe}$  capture, transitions to high spin and unassigned states not observed in thermal capture imply higher  $l$ -wave capture at a number of energies. Reduced width values suggest d-wave capture as the most likely explanation. However, other evidence shows that p-wave capture and anomalously strong M1 and E2 transitions occur in this region.

The distribution of reduced widths for low spin transitions in  $^{57}\text{Fe}$  is consistent with statistical behaviour for weaker transitions and some direct effects for the strongest transitions.

## VII. ACKNOWLEDGMENTS

This experiment was one of a series in the mass range  $A = 40$ –70 carried out by Dr. J. R. Bird, Mr. B. J. Allen, and the author at the A.A.E.C. Research Establishment, with assistance in individual experiments by Mr. G. J. Broomhall, Mr. D. M. H. Chan, and Mr. B. B. V. Raju of the University of Melbourne. The author is grateful for assistance in data collection and for discussions with these people and for the support of the members of the 3 MeV accelerator group.

## VIII. REFERENCES

- ALLEN, B. J. (1970).—AAEC Rep. No. TM565.  
 ALLEN, B. J., BIRD, J. R., and KENNY, M. J. (1969).—AAEC Rep. No. E200.  
 ALLEN, B. J., KENNY, M. J., and SPARKS, R. J. (1968).—*Nucl. Phys. A* **123**, 220.  
 ASAMI, A., MOXON, M. C., and STEIN, W. E. (1969).—*Phys. Lett. B* **28**, 656.  
 BARTHOLOMEW, G. A. (1961).—*Am. Rev. nucl. Sci.* **11**, 259.  
 BARTHOLOMEW, G. A., *et al.* (1967).—*Nucl. Data A* **3**, 367.  
 BIRD, J. R. (1968).—*Nucl. Phys. A* **120**, 113.

- BIRD, J. R., KENNY, M. J., and ALLEN, B. J. (1969).—AAEC Rep. No. TM511.
- BLOCK, R. C. (1964).—*Phys. Lett.* **13**, 234.
- BROOMHALL, G. J. (1972).—Capture of 10–100 keV neutrons in isotopes of titanium. *Aust. J. Phys.* **25** (in press).
- CHRIEN, R. E., BHAT, M. R., and WASSON, O. A. (1970).—*Phys. Rev. C* **1**, 973.
- GOLDBERG, M. D., MUGHABGHAB, S. F., MAGURNO, B. A., and MAY, V. M. (1966).—Brookhaven National Lab. Rep. No. BNL325.
- GROSHEV, L. V., DEMIDOV, A. M., KOTELNIKOV, G. A., and LUTSENKO, V. N. (1964).—*Nucl. Phys.* **58**, 465.
- HOCKENBURY, R. W., BARTOLOME, Z. M., TATARCZUK, J. R., MOYER, W. R. and BLOCK, R. C. (1969).—*Phys. Rev.* **178**, 1746.
- KENNY, M. J., BIRD, J. R. and ALLEN, B. J. (1969).—Proc. Int. Conf. on Properties of Nuclear States, Montreal, Contrib. L2.
- WASSON, O. A., GARG, J. B., CHRIEN, R. E., and BHAT, M. R. (1968).—Brookhaven National Lab. Rep. No. BNL12268.

